MOLECULAR AND CELLULAR BIOLOGY, Jan. 2004, p. 550–560 Vol. 24, No. 2
0270-7306/04/$08.00+0 DOI: 10.1128/MCB.24.2.550–560.2004

Early Glomerular Filtration Defect and Severe Renal Disease in Podocin-Deficient Mice

Séverine Roselli,[1] Laurence Heidet,[1] Mireille Sich,[1] Anna Henger,[2] Matthias Kretzler,[2] Marie-Claire Gubler,[1] and Corinne Antignac[1,3]*

INSERM U574, Hôpital Necker-Enfants Malades, Université René Descartes,[1] and Service de Génétique, Hôpital Necker-Enfants Malades,[3] Paris, France, and Nephrology Center, University of Munich, Munich, Germany[2]

Received 7 August 2003/Returned for modification 23 September 2003/Accepted 8 October 2003

Podocytes are specialized epithelial cells covering the basement membrane of the glomerulus in the kidney. The molecular mechanisms underlying the role of podocytes in glomerular filtration are still largely unknown. We generated podocin-deficient (*Nphs2*$^{-/-}$) mice to investigate the function of podocin, a protein expressed at the insertion of the slit diaphragm in podocytes and defective in a subset of patients with steroid-resistant nephrotic syndrome and focal and segmental glomerulosclerosis. *Nphs2*$^{-/-}$ mice developed proteinuria during the antenatal period and died a few days after birth from renal failure caused by massive mesangial sclerosis. Electron microscopy revealed the extensive fusion of podocyte foot processes and the lack of a slit diaphragm in the remaining foot process junctions. Using real-time PCR and immunolabeling, we showed that the expression of other slit diaphragm components was modified in *Nphs2*$^{-/-}$ kidneys: the expression of the nephrin gene was downregulated, whereas that of the ZO1 and CD2AP genes appeared to be upregulated. Interestingly, the progression of the renal disease, as well as the presence or absence of renal vascular lesions, depends on the genetic background. Our data demonstrate the crucial role of podocin in the establishment of the glomerular filtration barrier and provide a suitable model for mapping and identifying modifier genes involved in glomerular diseases caused by podocyte injuries.

Glomeruli are specialized structures responsible for blood filtration in the kidney and are targets of injury in a number of human diseases. Plasma ultrafiltration occurs through the glomerular filtration barrier, which is composed of highly specialized visceral epithelial cells called podocytes, a fenestrated capillary endothelium, and an intervening glomerular basement membrane (GBM) (28). Podocytes are octopus-like cells (18), comprising a cell body and cytoplasmic extensions called major processes, which divide into actin-rich foot processes interdigitating over each capillary loop and counteracting the distensive forces. Each foot process is attached to its neighbor along its length by an intercellular adherens-type junction (46), the slit diaphragm (SD), which is located just above the GBM. The recent discovery of several novel podocyte proteins and the description of their physical and functional interactions highlighted the critical role of the SD complex and of the actin cytoskeleton in the maintenance of the glomerular filtration barrier (34, 39; reviewed in references 31 and 41).

Glomerular diseases are associated with leakage of proteins across the filter into the urine and with disappearance (effacement) of podocyte foot processes. Whether effacement of foot processes is the cause or consequence of the glomerular filter alterations is uncertain. However, in renal diseases progressing toward focal and segmental glomerulosclerosis (FSGS), podocytes are now thought to be the primary targets, responsible for the development of the lesion. FSGS is characterized by segmental sclerotic lesions involving only a subpopulation of glomeruli and is a frequent cause of renal failure. It either represents a primary (idiopathic) condition or occurs in the course of several identified disorders, including human immunodeficiency virus infection, diabetes, renal mass reduction, and hypertension (10, 25).

We identified the podocin gene, *NPHS2*, as being involved in a familial form of early-onset steroid-resistant nephrotic syndrome progressing toward FSGS (3). Mutations in *NPHS2* are also associated with sporadic cases of the disease and with late-onset inherited FSGS (5, 6, 14, 29, 35, 57). Podocin is a stomatin-like protein, predicted to have a hairpin structure. Within the kidney, it is exclusively expressed in podocytes (3, 48). An oligomeric form of this membrane-anchored protein accumulates in lipid rafts at the insertion of the SD and interacts with other key components of the SD such as nephrin, CD2AP, and NEPH1 (23, 51, 52). These data suggest that podocin acts as a scaffolding protein, triggering SD assembly, although its precise role in the establishment and maintenance of the glomerular filtration barrier has not been completely elucidated. As a further step in determining the function of podocin, we generated mice lacking podocin by gene targeting in embryonic stem (ES) cells.

MATERIALS AND METHODS

Genomic structure of *Nphs2* and generation of the targeting construct. The partial cDNA sequence of the mouse *Nphs2* gene was found by searching the GenBank expressed sequence tag database (accession number AW106985). The remaining sequence was determined by analyzing the sequence of the corresponding IMAGE clone (clone IMAGE 2192627), generating the complete 3.1-kb *Nphs2* cDNA sequence. A PCR-generated cDNA probe spanning exons 1 to 4 was used to screen a 129/Sv Ev Tac flor genomic phage library in λFixII (Stratagene, La Jolla, Calif.) as previously described (7). One clone containing the full 20-kb *Nphs2* gene sequence was identified and purified. The mouse *Nphs2* gene consists of eight exons. Transcription gives rise to a 3.1-kb *Nphs2*

* Corresponding author. Mailing address: INSERM U574, Tour Lavoisier, 6ème Étage, Hôpital Necker-Enfants Malades, 75743 Paris, Cedex 15, France. Phone: 33-1-44-49-50-98. Fax: 33-1-44-49-02-90. E-mail: antignac@necker.fr.

mRNA, which encodes a 385-amino-acid protein that is 92% similar to human podocin. The genomic library was subsequently screened with a genomic probe corresponding to a 536-bp sequence located upstream from exon 1. This led to the identification of one 14-kb clone, starting ca. 8 kb upstream from the *Nphs2* putative transcription start site. The exon-intron structure was determined by restriction mapping and sequencing. The targeting construct was generated in three steps by using a floxed selection cassette (56) containing the hygromycin gene driven by a phosphoglycerate kinase promoter (PGK-Hyg), kindly provided by Marco Giovannini (Paris, France). First, the 3′ arm of homology, corresponding to a 6-kb *Hin*dIII fragment encompassing *Nphs2* exons 3 and 4, was inserted into pBluescript II SK(+/−) (Stratagene). The 5′ arm of homology, spanning a 3-kb DNA sequence upstream from exon 1, was PCR amplified with the primers 5′-TTGCGGCCGCGGACAACAAAGATGTATT-3′ and 5′-TTCGGCCGAC CGCTATGTGGATGCTG-3′ containing a *Not*I and an *Eag*I restriction site, respectively. The resulting fragment was inserted into the *Not*I site of the multiple cloning site of the previous construct. A *Not*I restriction site was added at the 3′ end of the insert by site-directed mutagenesis (QuikChange site-directed mutagenesis kit; Stratagene). Finally, the floxed PGK-Hyg selection cassette was subcloned into the *Sma*I site of the plasmid in the reverse orientation. The final construct was cut with *Not*I and purified by electroelution.

Generation of podocin-deficient mice. ES cells were electroporated with the targeting construct and selected for resistance to hygromycin (50 μg/ml). Electroporation of ES cells, microinjection into blastocysts and production of germ line-transmitting chimeras were performed by GenOway (Lyon, France). All procedures involving animals were conducted in accordance with national guidelines and institutional policies. Male chimeras were crossed with wild-type females. Heterozygous offspring were intercrossed to produce homozygous F_1 animals. Tail biopsies from F_1 animals were genotyped by PCR, the results of which were confirmed, in some cases, by Southern blot analysis. F_2 animals were mostly analyzed by PCR (30 PCR cycles of 1 min at 94°C, 1 min at 55°C, and 1 min at 72°C). The mutant allele was detected by the primers 5′-TTCATATGC GCGATTGCTGA-3′ and 5′-CCACGGCCTCCAGAAGAAGA-3′ located in the selection cassette. The wild-type allele was identified by the primers 5′-GC TGTCCTAGATGGGAAGT-3′ and 5′-TGCATACCTGGTGCCTATA-3′ located upstream of exon 1.

RNA and real-time RT-PCR analysis. Kidneys were snap-frozen in liquid nitrogen, and total RNA was extracted by use of an RNeasy kit (Qiagen, Inc., Valencia, Calif.) according to the manufacturer's instructions. Northern blot analysis was performed as previously described (7). Real-time reverse transcription-PCR (RT-PCR) analysis was performed as previously described (9). The following primers and probes were purchased from Applied Biosystems: α-actinin 4 primers 5′-AGTGCATGGTCCCTCTTTGG-3′ and 5′-CGCTGAGAGC AATCACATCAA-3′; α-actinin 4 fluorescence-labeled probe (FAM) 5′-ACCA GCTGCTGCACCTTCTCCCA-3′, CD2AP (accession number AF077003) primers 5′-AAACCACCTCCTCCTGCAAA-3′ and 5′-GCTTTCTTCTCTGCA GCTGACA-3′, CD2AP fluorescence-labeled probe (FAM) 5′-AGGTCCAGC TCCAAAG-3′; nephrin (accession number AF168466) primers 5′-ACCCTCCA GTTAACTTGTCTTTGG-3′ and 5′-ATGCAGCGGAGCCTTTGA-3′, nephrin fluorescence-labeled probe (FAM) 5′-TCCAGCCTCTCTCC-3′; P-cadherin primers 5′-GCTCTACCACGACGGCAGAG-3′ and 5′-GCCTCATACTTCTG CGGCTC-3′, P-cadherin fluorescence-labeled probe (FAM) 5′-CCTTGATGC CAACGATAACGCTCCG-3′; podoplanin primers 5′-TGTGCTTGCTGCCTC TGC-3′ and 5′-AGCTCGGGAGGAGGTTGG-3′, podoplanin fluorescence-labeled probe (FAM) 5′-CCCGGGCACTCTCTGGCGC-3′, synaptopodin (accession number XM_148853) primers 5′-TTCCTTGCCCTCACTGTTCT G-3′ and 5′-TCCTAGCAGCAATCCACATCTG-3′, and synaptopodin fluorescence-labeled probe (FAM) 5′-CCTAGCTTTCTAAAGGAC-3′; the 18S rRNA sequence (GenBank accession number XM_148853) was used to design the predeveloped TaqMan assay reagents. Controls consisting of H_2O were negative in all runs.

Urine and plasma analysis. Blood and urine were collected from deeply anesthetized mice by cardiac and bladder puncture, respectively. Blood urea nitrogen levels were measured on a Hitachi model 917 automatic analyzer (Tokyo, Japan). Urinary proteins were analyzed by sodium dodecyl sulfate-polyacrylamide gel electrophoresis (SDS-PAGE), followed by Coomassie blue staining.

Histologic analysis. Kidneys were removed from killed mice, fixed in Dubosq-Brazil or formalin, dehydrated, and embedded in paraffin. Sections (3 μm) were stained with hematoxylin and eosin, trichrome light green, and periodic acid with hematoxylin. Sections were examined under a Leitz Orthoplan microscope (Leica Microscopic Systems, Heezbrugg, Switzerland).

For electron microscopy, tissue samples were processed as previously described (7). Tissue specimens from littermate controls (*Nphs2*$^{+/+}$ or *Nphs2*$^{+/-}$ mice) were systematically processed and examined in the same conditions.

Immunohistology. (i) Immunofluorescence staining. Tissues were snap-frozen in liquid nitrogen by using a CRYO-M-BED (Miles Laboratories, Inc., Naperville, Ill.) and stored at −80°C until use. Immunofluorescence labeling was performed as previously described (48). For collagen labeling, slides were treated with 6 M urea-glycine (pH 3.5) before being incubated with the primary antibody. A Mouse-to-Mouse kit (M.O.M.; Vector Laboratories, Burlingame, Calif.) was used to detect mouse primary antibodies. Labeled samples were examined with a Leitz Orthoplan microscope (Leica Microscopic Systems).

(ii) Antibodies. Affinity-purified antibodies recognizing [$(\alpha1)_2\alpha2$] collagen IV protomers, raised against pepsin-digested human placenta type IV collagen, were obtained from Novotec (Lyon, France). Rabbit antibodies against nephrin, α3-integrin, laminin α2 and laminin α5 were generous gifts from K. Tryggvason, R. Hynes, P. Yurchenco, and J. Miner, respectively. Rat monoclonal antibodies (MAbs) to α1, β1, and γ1 laminin chains, entactin-nidogen, and perlecan were purchased from Chemicon International (Temecula, Calif.). Rabbit anti-CD2AP antibodies, goat anti-agrin antibodies (Santa Cruz Biotechnology, Santa Cruz, Calif.), rabbit anti-ZO1 (Zymed Laboratories, San Francisco, Calif.), anti-fibronectin MAbs (Novotec, Lyon, France), mouse anti-α3(IV) collagen (Wieslab AB, Lund, Sweden), anti-synaptopodin (PROGEN Biotechnik, Heidelberg, Germany), and anti-α-smooth muscle actin (αSMA) MAbs (Sigma, St. Louis, Mo.) were used according to the manufacturers' recommendations. Primary antibodies were detected with either fluorescein isothiocyanate-conjugated donkey anti-rabbit immunoglobulin G (IgG) or Cy2-conjugated donkey anti-rat, anti-goat, or anti-mouse IgG.

(iii) Double immunofluorescence labeling and confocal microscopy. For dual fluorochrome labeling, the slides were simultaneously incubated with rabbit anti-nephrin antibodies and rat anti-nidogen antibodies as previously described (4). After a wash with phosphate-buffered saline, the slides were incubated with an unlabeled goat anti-rat serum. The slides were washed again in phosphate-buffered saline and then incubated simultaneously with Cy2-conjugated donkey anti-rabbit IgG and Cy3-conjugated donkey anti-goat IgG. Sections were examined with a Zeiss confocal microscope (Carl Zeiss, Jena, Germany).

Statistical analyses. The values reported are the means ± the standard error of the mean. Statistical comparisons were performed by using either the Student *t* test or the Mann-Whitney test as appropriate. *P* values of <0.05 were considered significant.

RESULTS

Generation of mice lacking podocin. We disrupted the *Nphs2* gene in 129/Sv ES cells by homologous recombination with a targeting vector in which a genomic fragment spanning exons 1 and 2 and the putative transcription start site was replaced by a floxed PGK-Hyg cassette (Fig. 1a). Two of the five correctly targeted ES clones were injected into C57BL/6J blastocysts. One of these two clones produced chimeras. Male chimeras were crossed either with C57BL/6J or with 129/Sv wild-type females, producing heterozygous offspring (*Nphs2*$^{+/-}$) with a mixed C57BL/6J-129/Sv (strain B6/129) or a pure 129/Sv (strain 129) genetic background, respectively. *Nphs2*$^{+/-}$ mice from either genetic background were intercrossed to produce homozygous knockout mice (*Nphs2*$^{-/-}$). The disruption of *Nphs2* was verified by Southern blot (Fig. 1b). To confirm that *Nphs2* had been correctly inactivated, we performed Northern blot and immunofluorescence experiments, which showed the absence of podocin transcripts (Fig. 1c) and protein (Fig. 1d) in *Nphs2*$^{-/-}$ kidneys, respectively.

***Nphs2*$^{-/-}$ mice display congenital proteinuria and renal failure, the progression of which depends on the genetic background.** *Nphs2*$^{+/-}$ mice did not show any gross abnormalities. Their renal function was normal and urine analysis showed the absence of albuminuria. These mice have currently been followed up for 12 months. Light microscopic examination of *Nphs2*$^{+/-}$ mice did not show any abnormalities at that time. Genotyping at birth showed that 26.6% (8 of 30) of the pups born after *Nphs2*$^{+/-}$ intercrosses were *Nphs2*$^{-/-}$. This finding

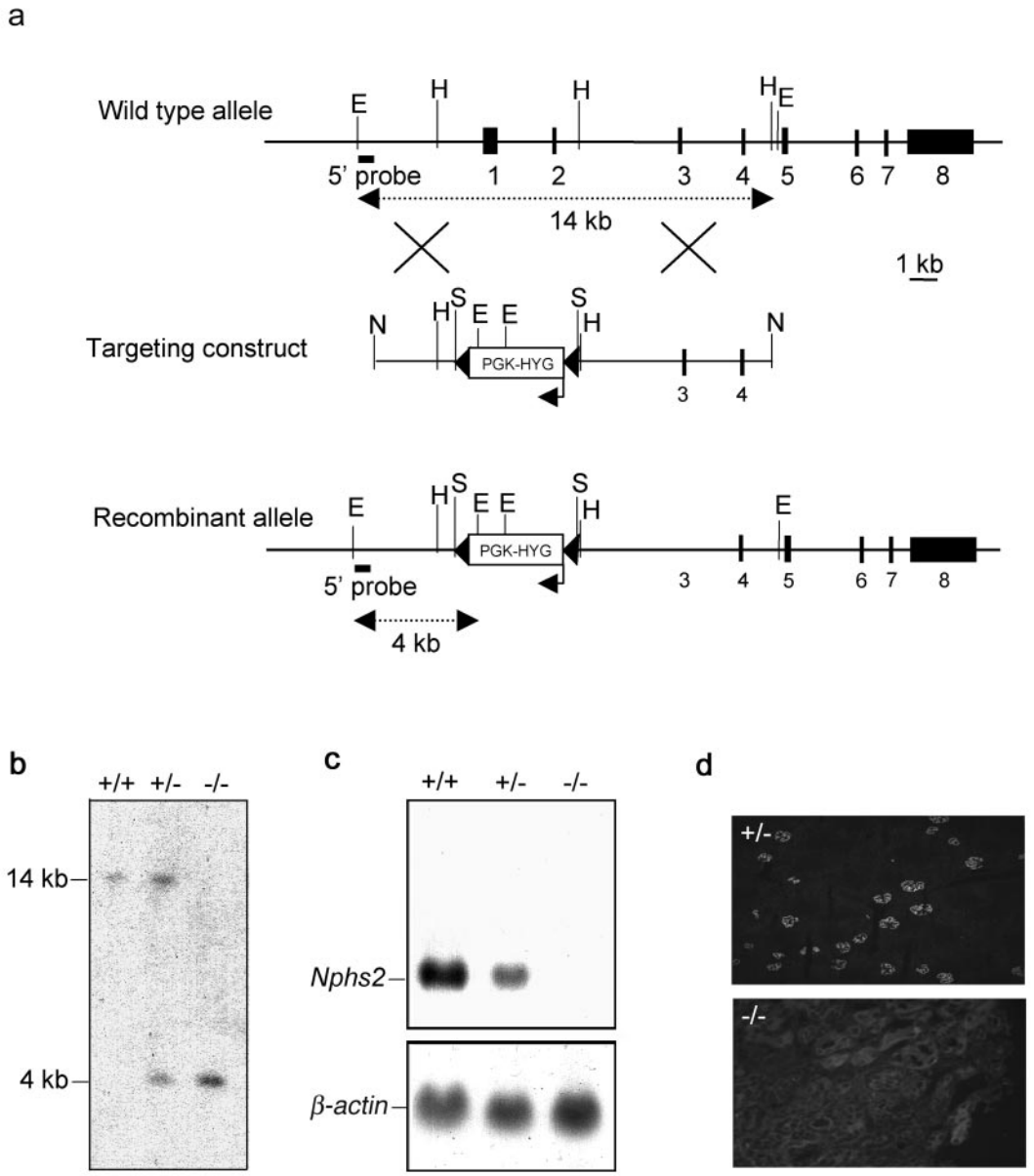

FIG. 1. Disruption of the *Nphs2* gene. (a) Schematic representation of the genomic structure of the wild-type murine *Nphs2* allele (top), the targeting construct (middle), and the targeted allele (bottom). The eight exons are represented by closed boxes. The region containing exons 1 and 2 was replaced by a floxed PGK-hygromycin cassette (PGK-HYG) (the arrow indicates the orientation of this gene). The LoxP sites are represented by black arrowheads. Restriction enzyme cleavage sites are indicated (E, *Eco*RI; H, *Hin*dIII, S, *Sma*I, N, *Not*I). (b) Southern blot analysis of genomic DNA from *Nphs2*$^{+/+}$, *Nphs2*$^{+/-}$, and *Nphs2*$^{-/-}$ mice with a 5′-external probe (solid bar). The 14-kb wild-type *Eco*RI fragment was detected in the *Nphs2*$^{+/+}$ mouse; the recombinant 4-kb fragment, created due to the presence of an *Eco*RI site in the cassette, was detected in the *Nphs2*$^{-/-}$ mouse, and both bands were detected in the *Nphs2*$^{+/-}$ mouse. (c) Northern blot analysis of 20 μg of total kidney RNA from *Nphs2*$^{+/+}$, *Nphs2*$^{+/-}$, and *Nphs2*$^{-/-}$ mice hybridized with a 3′ cDNA probe spanning exons 4 to 8. The endogenous 3.1-kb *Nphs2* transcript was detected in *Nphs2*$^{+/+}$ mice, no transcript was detected in *Nphs2*$^{-/-}$ mice due to the deletion of the transcription start site, and the endogenous 3.1-kb transcript was detected in *Nphs2*$^{+/-}$ mice, although the band was weaker than in *Nphs2*$^{+/+}$ mice. (d) Immunofluorescence study on cryostat sections of kidneys from *Nphs2*$^{+/-}$ and *Nphs2*$^{-/-}$ mice with a rabbit anti-human antibody directed against the C-terminal part of podocin. Podocin was detected in the glomeruli of *Nphs2*$^{+/-}$ mice, whereas no signal was observed in the *Nphs2*$^{-/-}$ kidney, a finding consistent with the lack of *Nphs2* transcripts.

is consistent with classic Mendelian segregation and strongly suggests the absence of prenatal mortality. Although they appeared to be normal at birth, *Nphs2*$^{-/-}$ mice rapidly presented growth retardation and died in the first 5 weeks of life. Interestingly, death occurred much later in the 129 background than in the mixed B6/129 background (22.7 ± 1.5 days [$n = 10$] versus 7.4 ± 1.5 days [$n = 22$], respectively; $P < 0.0001$) (Fig. 2a). Litter sizes were similar in the two backgrounds. Macroscopically, kidneys from B6/129 *Nphs2*$^{-/-}$ mice were of normal size at the time of death but presented red spots due to local-

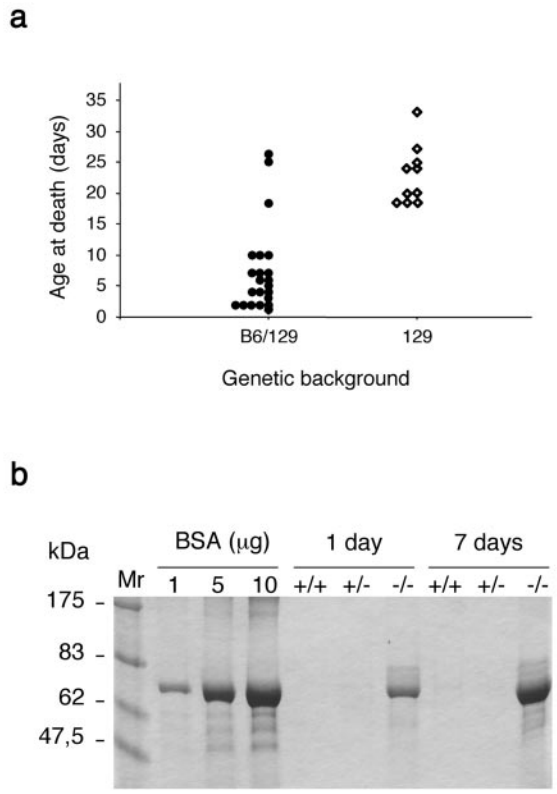

FIG. 2. Clinical features of *Nphs2*$^{-/-}$ *mice.* (a) Schematic representation of the survival of *Nphs2*$^{-/-}$ mice from the mixed B6/129 and the pure 129 genetic backgrounds; (b) SDS-PAGE analysis of urine from *Nphs2*$^{+/+}$, *Nphs2*$^{+/-}$, and *Nphs2*$^{-/-}$ B6/129 littermates (1 and 7 days old). One microliter of urine from each mouse and albumin standards were loaded on the same gel. Massive proteinuria, mainly consisting of albumin, was observed in *Nphs2*$^{-/-}$ mice from birth but not in control mice.

ized hemorrhage (Fig. 3a). However, these gross abnormalities were never observed in 129 *Nphs2*$^{-/-}$ animals.

SDS-PAGE analysis of urine from *Nphs2*$^{-/-}$ mice showed severe proteinuria, mainly consisting of albumin (Fig. 2b). In fact, massive proteinuria was present from birth in both types of *Nphs2*$^{-/-}$ mouse, although these animals were macroscopically indistinguishable from their littermates at this age. At death, the blood urea nitrogen (59.49 ± 14.72 μmol/liter versus 6.58 ± 0.69 mmol/liter; $P = 0.0027$) and creatinine (95.00 ± 26.93 μmol/liter versus 22.33 ± 3.80 μmol/liter; $P = 0.0019$) concentrations were significantly higher in plasma from *Nphs2*$^{-/-}$ mice ($n = 8$) than in plasma from *Nphs2*$^{+/+}$ littermates ($n = 8$). Thus, mice lacking podocin died with end-stage renal failure.

***Nphs2*$^{-/-}$ mice develop massive mesangial sclerosis.** Kidneys from 16 *Nphs2*$^{-/-}$ mice (1 to 25 days old) of the mixed genetic background and 14 *Nphs2*$^{-/-}$ mice (1 to 33 days old) of the pure genetic background were analyzed by light microscopy. Since the stepwise induction of new nephrons in the mouse continues until approximately 2 weeks after birth, sections of early postnatal kidneys contain nephrons at all stages of development. Microscopic examination of *Nphs2*$^{-/-}$ kidneys showed that the different steps of nephrogenesis were normal and confirmed that the predominant renal changes involved the glomeruli. Unexpectedly, *Nphs2*$^{-/-}$ mice did not show FSGS lesions but displayed typical features of diffuse mesangial sclerosis (DMS), the progression of which depends on the genetic background. The mature glomeruli in B6/129 *Nphs2*$^{-/-}$ mice were markedly bigger than those of their wild-type littermates due to the accumulation of the mesangial matrix without mesangial cell proliferation (Fig. 3b to d). Podocytes were enlarged and focally vacuolized. Those vacuoles were stained with an antibody directed against albumin (data not shown). Mesangial sclerosis and occasional mesangiolysis rapidly progressed with age and massively involved all mature glomeruli, reducing the patency of the capillary lumens. Completely sclerotic glomeruli were still surrounded by a layer of hypertrophied podocytes and did not adhere to the Bowmann's capsule. Whereas various degrees of mesangial sclerosis were seen in all mature glomeruli of the deep cortex, the small and immature glomeruli of the immediate subcapsular zone appeared to be initially preserved, and mild mesangial sclerosis was also seen in immature glomeruli in mice surviving longer than 10 days. Glomerular lesions were associated with tubular changes involving primarily proximal tubules and characterized by focal dilatations, vacuolization of the epithelium, and the presence of protein casts. These lesions were seen in fully developed proximal tubules, even when glomerular changes were still mild to moderate, as early as on postnatal day 1. Interestingly, one B6/129 *Nphs2*$^{-/-}$ mouse killed on day 25 and displaying heavy proteinuria showed normal renal function and mesangial sclerosis that was focal and associated with severe tubular dilatation.

Very severe arteriolar lesions characterized by marked thickening of the arteriolar wall, endothelial cell hypertrophy, diffuse dilatation of peritubular capillaries, and multiple foci of interstitial hemorrhages predominating in the superficial cortex were observed as early as day 2 in B6/129 *Nphs2*$^{-/-}$ mice (Fig. 3b). The thickening of the arteriolar wall was emphasized by the presence of several layers of αSMA-positive muscular cells (Fig. 3e and f). Arcuate arteries, which are larger in diameter, were not affected.

In the pure 129 background, renal arteries were normal, and no interstitial hemorrhages were observed. The glomerular lesions were most often similar to those described in B6/129 *Nphs2*$^{-/-}$ but developed less rapidly. Curiously, another type of glomerular change was prominent in two mice (the first two mice examined, which were 24 and 27 days old). This change consisted of the retraction and collapse of the glomerular tuft lined by huge vacuolized podocytes, the number of which appeared increased, suggesting epithelial cell proliferation. These glomeruli did not display any mesangial matrix accumulation (Fig. 3g and h). The proximal tubule was dramatically and diffusely dilated in these two mice with collapsing nephropathy. Finally, unlike in B6/129 *Nphs2*$^{-/-}$ animals, superimposed crescentic lesions involving 5 to 40% of the glomeruli were present from day 13 in 129 *Nphs2*$^{-/-}$ mice, whatever the type of the underlying glomerular change (Fig. 3i and j).

***Nphs2*$^{-/-}$ mice lack an SD.** Kidneys from five *Nphs2*$^{-/-}$ mice or embryos (embryonic day 16.5 [E16.5] and 1, 4, and 6 days old) of the mixed B6/129 genetic background and from four *Nphs2*$^{-/-}$ mice or embryos (E16.5 and 1, 8, and 25 days

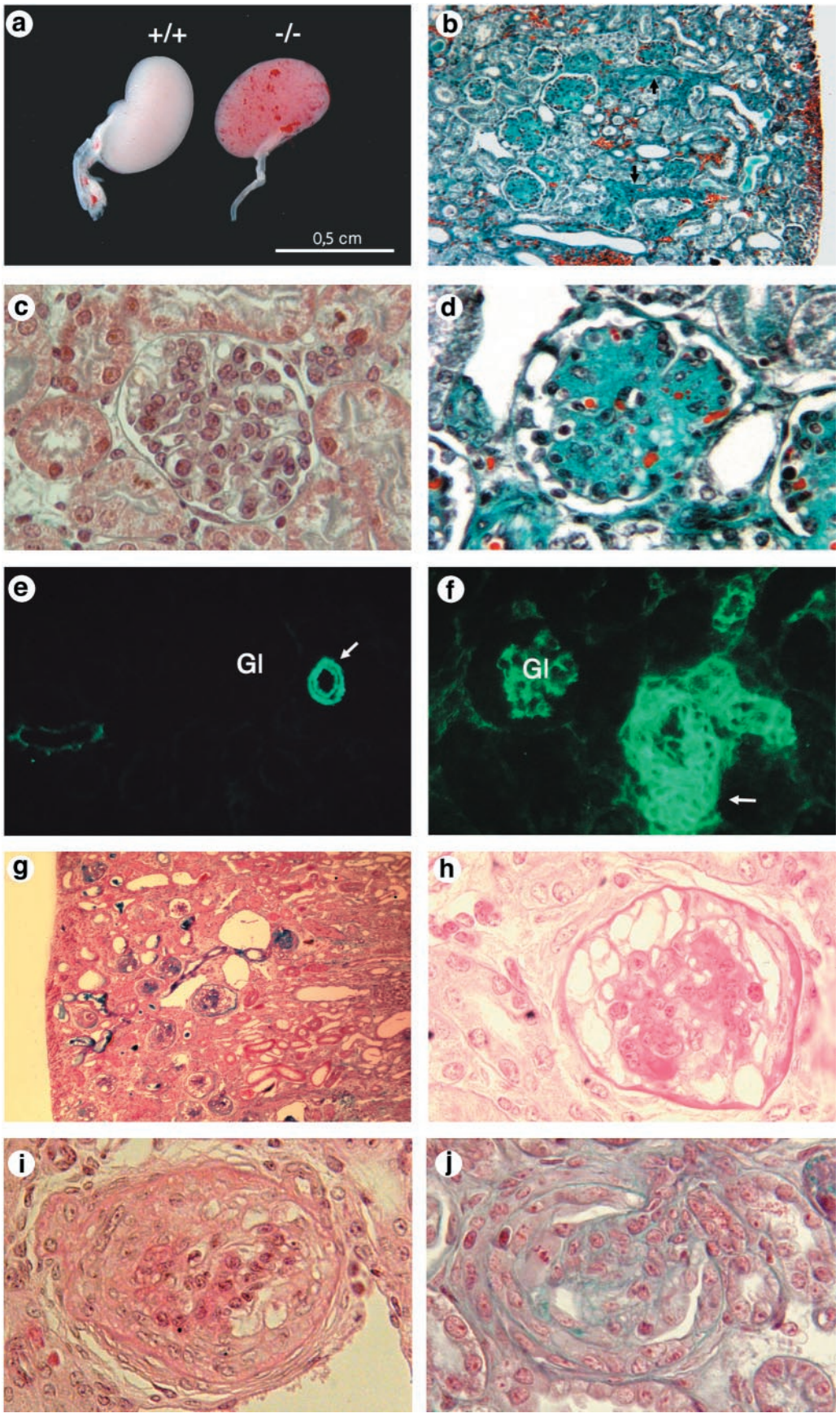
a
+/+
-/-
0,5 cm
b
c
d
e
Gl
f
Gl
g
h
i
j

old) of the pure 129 genetic background were studied by electron microscopy. Podocyte changes were essentially the same in both backgrounds. They consisted of extensive effacement of foot processes and microvilli formation. Both of these changes could be observed from E16.5 in mature glomeruli and persisted after birth, focally associated with cytoplasmic vacuolization (Fig. 4a and b). Some foot processes were preserved. They were enlarged and located close together and had no visible SD, in contrast to the regular spacing and normal organization of foot processes in wild-type mice (Fig. 4c and d). The occasional interpodocyte junctions appeared as close contact areas that lacked SDs. The accumulation of mesangial matrix material became apparent on day 2 in the B6/129 *Nphs2*$^{-/-}$ mice, progressed with age, and was focally associated with clear areas of mesangiolysis (Fig. 4e). Impressive podocyte vacuolization was seen in the collapsing form of glomerulopathy (Fig. 4f).

The expression of several podocyte genes is modified in *Nphs2*$^{-/-}$ mice. Since podocin is thought to act as a scaffolding molecule for the SD complex, we studied the expression level and the cellular localization of some of the key components of the SD complex. Kidneys from three *Nphs2*$^{+/+}$ mice and three *Nphs2*$^{-/-}$ mice (10 days old) of the pure 129 genetic background were analyzed by real-time PCR and immunostaining. Nephrin, the protein that is defective in the congenital nephrotic syndrome of the Finnish type (32), is a transmembrane immunoglobulin-like protein thought to be a major component of the filtration slit (21, 49). Nephrin mRNA levels were three times lower in *Nphs2*$^{-/-}$ mice than in wild-type mice (Table 1). The nephrin labeling shifted from a linear pattern in the control animals to a granular pattern, with irregular extensions at some distance from the GBM, in *Nphs2*$^{-/-}$ mice. Occasionally, the entire podocyte appeared to be labeled (Fig. 5a), a pattern that was confirmed by colabeling with antibodies directed against nidogen (a basement membrane protein) (Fig. 5a). The linear staining observed along the GBM in wild-type mice with antibodies directed against ZO1, a tight junction-associated protein also associated with the SD (50), was found more intense in *Nphs2*$^{-/-}$ mice than in *Nphs2*$^{+/+}$ mice (Fig. 5b). Furthermore, levels of CD2AP mRNA, an important SD-associated protein that is a cytosolic partner of nephrin and podocin (53, 54), showed a trend toward an mRNA induction (Table 1). CD2AP labeling was stronger in *Nphs2*$^{-/-}$ mice than in wild-type littermates (Fig. 5b). Consistent with unchanged mRNA levels, normal podocyte labeling was observed along the GBM in *Nphs2*$^{-/-}$ mice with antibodies to synaptopodin, an actin-associated protein found in podocyte foot processes. In addition, the immunolabeling of the α3 chain of the α3β1-integrin, a receptor for extracellular matrix components that is highly expressed at the site of adhesion of the podocytes to the GBM (Table 1 and Fig. 5b), was unchanged. Finally, the mRNA levels of the SD protein P-cadherin, the actin-binding molecule α-actinin 4, and the podocyte-specific transmembrane molecule podoplanin were not altered (Table 1).

Production of extracellular matrix proteins (Fig. 6). Due to the rapid progression to DMS observed in B6/129 *Nphs2*$^{-/-}$ mice, we studied the expression of several extracellular matrix proteins in these animals on days 4 and 6. High levels of nidogen and α5-laminin, two proteins that are normally only expressed in the GBM, were detected in the enlarged mesangial matrix in the *Nphs2*$^{-/-}$ mice, in addition to the expected linear staining of the GBM. In addition, the extension and intensity of mesangial labeling normally observed with antibodies to type IV collagen [α1(IV)2 α2(IV)], laminin chains α2, β1, and γ1, fibronectin, and perlecan were markedly increased in *Nphs2*$^{-/-}$ mice compared to wild-type littermates. The distribution and the staining intensity of the α3 chain of type IV collagen and of agrin (not shown), two proteins normally expressed in the GBM, were not modified in *Nphs2*$^{-/-}$ mice. However, as a consequence of the mesangial expansion, the GBM was pushed outward, resulting in a simplified, smoothly lobular pattern of labeling.

DISCUSSION

The SD complex is a modified adherens junction and contains at least four known transmembrane proteins: nephrin; NEPH1, which is structurally related to nephrin (11); P-cadherin (46); and FAT, a large cadherin homolog (8, 26). At the intracellular insertion site of the SD, ZO1 and CD2AP associate with NEPH1 (24) and nephrin (53), respectively. Podocin, which is thought to be anchored to the plasma membrane, interacts in the SD area with CD2AP, nephrin (51), and NEPH1 (52). These proteins connect directly or indirectly the SD to the actin cytoskeleton (37, 59). It was shown recently that, in addition to its structural function, nephrin is involved in signal transduction (22, 23) and that podocin enhances nephrin mediated cellular signaling (23). The SD-associated protein complex thus appears to be a lipid raft signaling nexus, and tyrosine-phosphorylation of nephrin by Src family kinases (36, 55, 58) might play a crucial role in nephrin-mediated signal transduction.

We generated mice lacking podocin, which is defective in

FIG. 3. Histologic analysis of *Nphs2*$^{-/-}$ mice. (a to f) Mixed B6/129 genetic background. (a) Kidneys from *Nphs2*$^{+/+}$ and *Nphs2*$^{-/-}$ mice at 3 days of age. Red spots due to localized hemorrhages are visible at the surface of the *Nphs2*$^{-/-}$ mouse kidneys. (b) Diffuse glomerular involvement in a 7-day-old mouse associated with focal tubular dilatation, arteriolar thickening (arrow), and interstitial hemorrhages (magnification, ×180). (c) Normal mouse glomerulus (magnification, ×800). (d) Massive mesangial sclerosis in a 7-day-old mouse (magnification, ×720). (e and f) Immunohistochemical analysis of αSMA distribution. (e) In a 6-day-old wild-type mouse kidneys, αSMA labeling is strong in arterial and arteriolar smooth muscle cells (arrow) and negative in mature glomeruli (Gl). (f) In a 6-day-old *Nphs2*$^{-/-}$ mouse, marked thickening of the arterial wall is accentuated by the presence of several layers of αSMA-positive cells (arrow). In addition, high levels of αSMA were observed in mesangial cells of the glomeruli (Gl). (g and h) Collapsing form of glomerulopathy in one 24-day-old *Nphs2*$^{-/-}$ mouse of the pure 129 genetic background. (g) Presence of tubular dilatations and absence of vascular lesions (magnification, ×180). (h) Retraction of the glomerular tuft, and diffuse and massive podocyte vacuolization (magnification, ×720). (i and j) Superimposed crescentic lesions in a 24-day-old 129 *Nphs2*$^{-/-}$ mouse with a collapsing form of glomerulopathy (i) and in a 13-day-old 129 *Nphs2*$^{-/-}$ mouse with a sclerotic form of the disease (j).

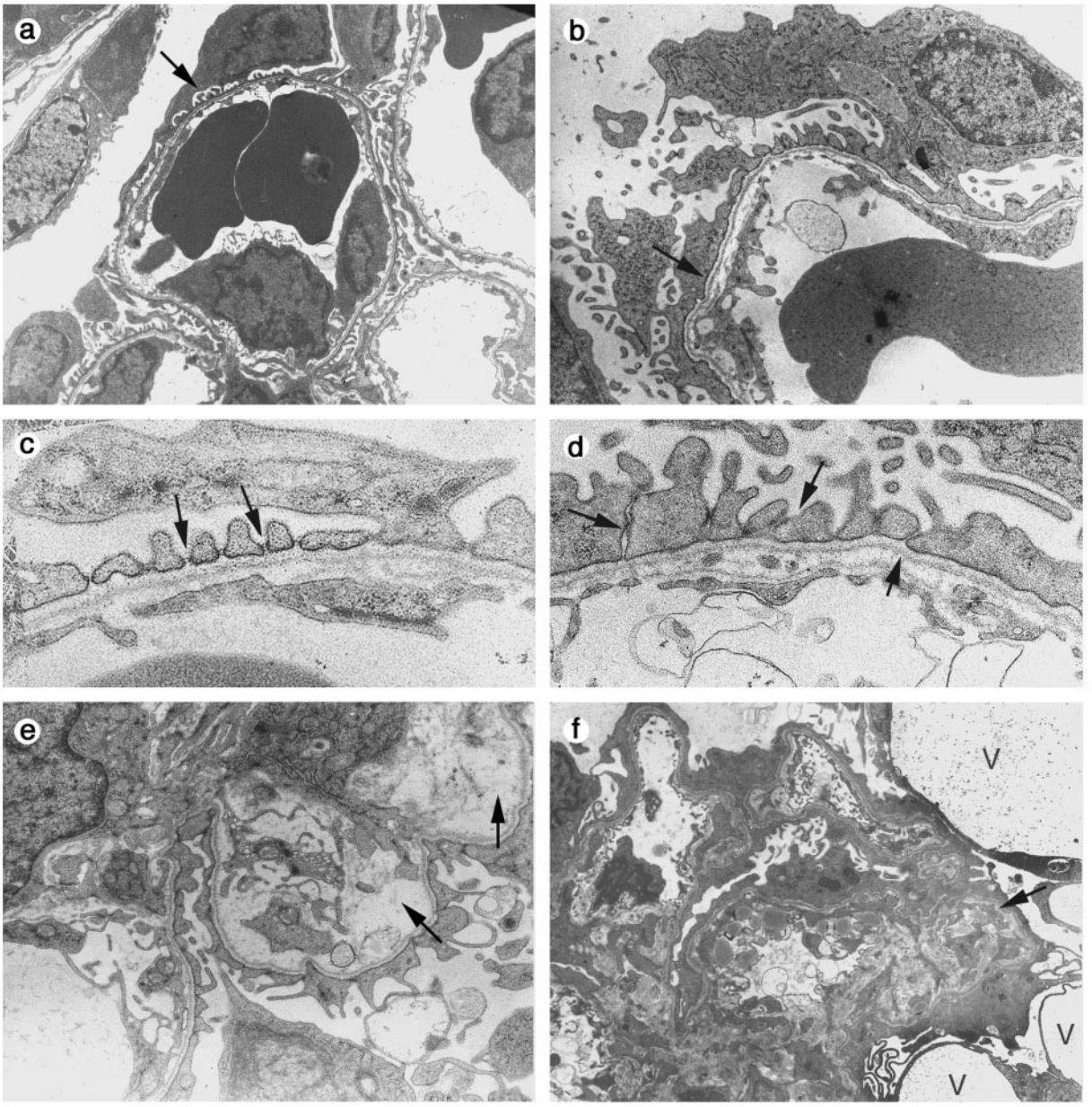

FIG. 4. Electron microscopy study of *Nphs2*$^{-/-}$ mice. (a to e) Mixed B6/129 genetic background. (a) Normal differentiation of foot processes (arrow) in a mature glomerulus of a 1-day-old wild-type mouse. (b) As a comparison, diffuse effacement of foot processes (arrow) in a 1-day-old *Nphs2*$^{-/-}$ mouse with podocyte microvilli formation is shown. (c) At high magnification, the SD (arrows) between regularly spaced foot processes is clearly visible in a 1-day-old wild-type mouse. (d) One-day-old *Nphs2*$^{-/-}$ mouse. Focally, foot processes are present in *Nphs2*$^{-/-}$ mice, but they are irregular in size and shape; the SD is replaced by irregular adhesions between adjacent cells (arrows). (e) Focal mesangiolysis (arrows) in a 7-day-old mouse. (f) 129 genetic background. Diffuse effacement of foot processes, collapse of the vascular tuft (arrow), and presence of large podocyte vacuoles (V) in a 24-day-old *Nphs2*$^{-/-}$ mouse. Magnifications: panels a and f, ×3,250; panels b and e, ×7,350; panels c and d, ×18,000.

familial and sporadic cases of nephrotic syndrome with FSGS in humans. *Nphs2*$^{-/-}$ mice produce urine but are massively proteinuric at birth. The kidneys develop normally in podocin-null mice: each step of nephrogenesis appeared to be normal, and kidney size at birth was similar to that in wild-type counterparts. However, podocyte foot processes were only occasionally seen by electron microscopy. They were abnormal and lacked SD. This finding, observed from E16.5, confirms that podocin is essential in the assembly of the SD complex and the maintenance of the glomerular filtration barrier. The disease progressed rapidly, and *Nphs2*$^{-/-}$ animals died in the first 5 weeks of life with end-stage renal failure caused by the development of DMS, characterized by massive mesangial accumulation of extracellular matrix proteins. None of the *Nphs2*$^{+/-}$ mice have developed proteinuria so far. Studies with a longer follow-up period will determine whether *Nphs2* haploinsufficiency plays a role in the long-term development of glomerular lesions, either spontaneously or in pathological situations such

TABLE 1. RNA levels of genes encoding podocyte components as ratios to 18 S rRNA

Genotype	Mean ratio (10^{-5}) ± SD[a]					
	Nephrin	CD2AP	α-Actinin 4	P-cadherin	Podoplanin	Synaptopodin
Nphs2$^{+/+}$	1.4 ± 0.39*	16 ± 1.6	26 ± 3.8	1.8 ± 0.27	0.33 ± 0.07	0.42 ± 0.21
Nphs2$^{-/-}$	0.54 ± 0.11*	22 ± 3.7	31 ± 14	3.2 ± 1.9	0.36 ± 0.07	0.51 ± 0.14

[a] $n = 3$ in each group. *, $P < 0.05$ (Student t test).

as nephron reduction. Such a susceptibility for glomerular alteration has been recently reported in association with CD2AP haploinsufficiency (33).

Thus, the phenotype of podocin-null mice is different and more severe than that of humans carrying *NPHS2* mutations. Patients are usually not proteinuric at birth and progress more slowly to end-stage renal disease through the development of FSGS but not DMS. In humans, DMS is mainly observed in patients carrying dominant-negative mutations of *WT1* (27, 44), a zinc-finger transcription factor expressed in podocytes. The finding of DMS in *Nphs2*$^{-/-}$ mice may have suggested that *NPHS2* is a target gene of WT1 and that DMS is a consequence of the podocin defect in affected humans. However, the study of patients affected with DMS not associated with a *WT1* mutation showed that DMS is not associated with *NPHS2* mutations (unpublished data). The differences in the severity of the disease and the type of glomerular lesions in *Nphs2*$^{-/-}$ mice and in humans may be because these mice completely lack podocin, whereas affected humans frequently carry the gene containing a missense mutation. We and others (42, 48a) have shown that, in vitro, many *NPHS2* missense mutations found in humans affect the trafficking of the protein and probably result in null-like alleles. However, we cannot rule out the possibility that a small amount of the mutant podocin reaches the podocyte cell membrane at the SD insertion site in patients in vivo. Conversely, the development of DMS in mice may be a more frequent response to injury in mouse glomeruli. In agreement with the last hypothesis is the remarkable severity and the frequent occurrence of DMS in mouse models of hereditary glomerular diseases associated with mutations in genes encoding podocyte proteins. Mice deficient for CD2AP (54) or NEPH1 (11) develop progressive mesangial sclerosis quite similar to the one observed in podocin-deficient mice. Similarly, donor splice site mutations of *WT1* intron 9, responsible for Frasier syndrome, a rare human disorder that associates FSGS and male to female sex reversal, also result in a more severe phenotype in mice (19), which display DMS but not FSGS. Altogether, these data support the hypothesis that DMS can develop as a consequence of podocyte injury. Our real-time PCR analysis revealed that the level of *Nphs1* mRNA was lower in *Nphs2*$^{-/-}$ mice than in their wild-type counterparts. Such an *Nphs1* downregulation was previously reported in mice that develop DMS because of a reduced expression level of WT1 (17). Interestingly, a mutant *Nphs1* mouse line shows glomerular lesions quite similar to the one we report here (45). This may suggest that nephrin is involved, in some way, in the development of DMS. On the other hand, similar transcriptional downregulation of *NPHS1* has been reported in humans affected with proteinuric nephropathies (15) and in mice developing an FSGS-like nephropathy due to the podocyte production of a mutant α-actinin 4 protein (39). In addition, the distribution of nephrin was modified in *Nphs2*$^{-/-}$ mice; it shifted from a linear to a granular pattern, and nephrin was localized at some distance from the GBM. This strongly suggests that podocin is required for the correct assembly of nephrin at the SD. Because of early death in podocin-deficient mice, we were not able to harvest sufficient *Nphs2*$^{-/-}$ podocyte material to check whether the absence of podocin affects the lipid raft localization of nephrin and SD-associated proteins and/or modifies nephrin signaling and phosphorylation. Alternatively, this nephrin staining pattern may be unspecifically related to proteinuria, since it has been observed in humans affected with nephrotic syndrome (12) and in animal models of induced proteinuria (30, 60). Immunofluorescence analysis showed that two other components of the SD complex, CD2AP and ZO1, seemed to be expressed at a higher level in podocin-deficient mice than in controls. Since CD2AP is expressed both in podocytes and in kidney tubules (38) and since we studied total kidney mRNA, a significant transcriptional upregulation of *Cd2ap* in the podocyte might have been overlooked. Interestingly, both *Cd2ap* and *Nphs2* are transcriptional targets of LMX1B, an LIM-homeodomain transcription factor expressed in podocytes (40, 47). Whether transcriptional or posttranscriptional, the upregulation of CD2AP was insufficient to compensate the glomerular filtration defect in *Nphs2*$^{-/-}$ mice.

Another important finding of our study was the difference in the rate of disease progression according to the genetic background. Mice lacking podocin reached end-stage renal failure more rapidly when they were from a mixed B6/129 background than when they were from a pure 129 genetic background. Another striking difference was the development of severe renal arteriolar lesions associated with subcapsular hemorrhages in the B6/129 background, whereas vessels appeared normal in 129 *Nphs2*$^{-/-}$ mouse kidneys. These lesions possibly developed as a consequence of severe hypertension. However, we were not able to measure blood pressure in these mice, which did not survive beyond 10 days. It is unlikely that these differences were caused by environmental factors, since all mice were bred together in the same animal house and the litter sizes were similar between the two backgrounds. This suggests the presence of modifier genes. Such genes have been suggested to act upon the progression of other glomerular diseases in humans and in animals (1, 2, 16, 43). Surprisingly, C57BL/6 mice have been shown to be resistant to glomerulosclerosis and arteriolar lesions after nephron reduction or hyperglycemia (13, 20, 61). This may suggest that genes modifying the course of glomerular diseases associated with podocyte injury are different from those involved in the progression of glomerulosclerosis due to nephron reduction. However, we

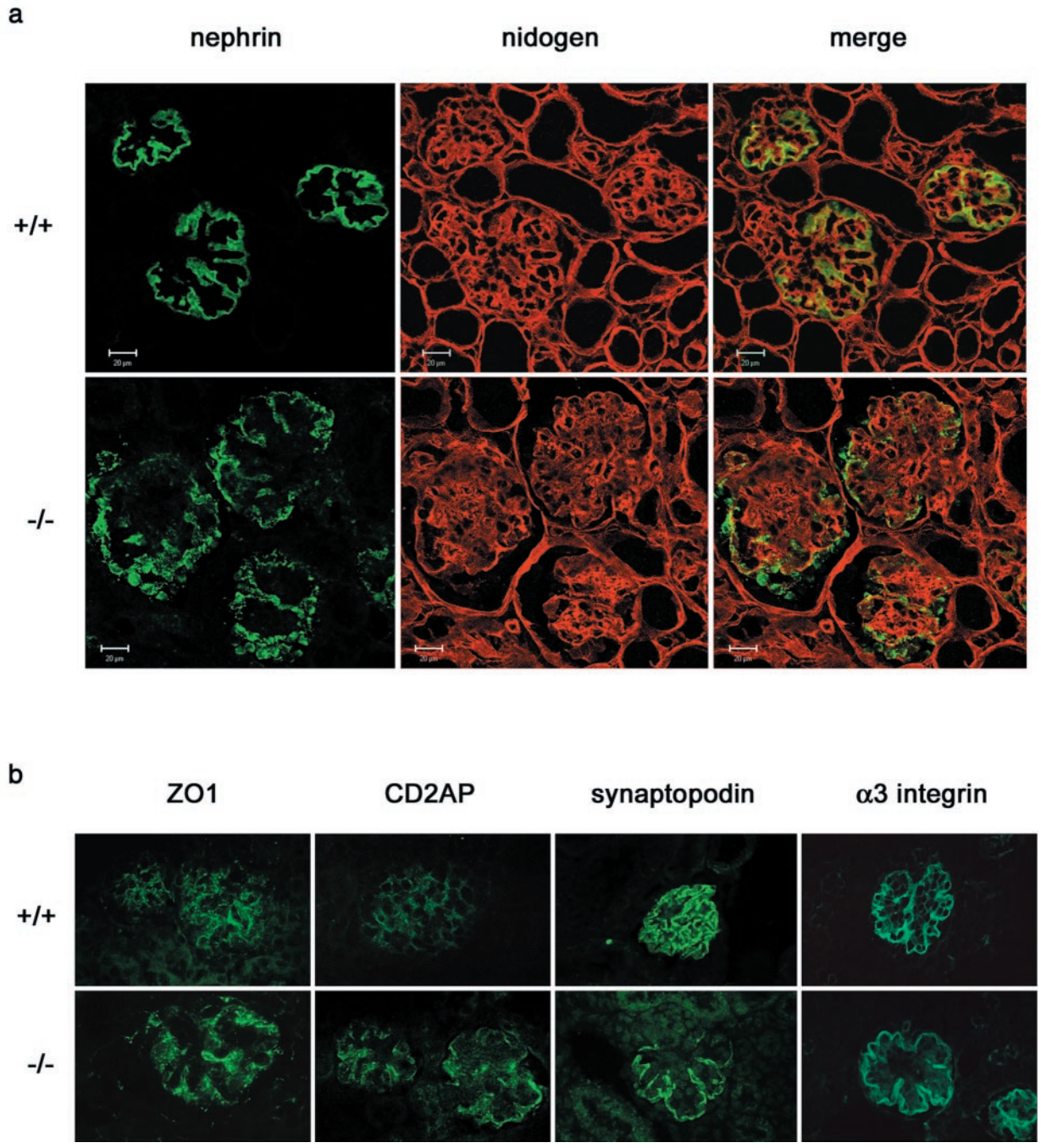

FIG. 5. Immunohistochemical analysis of the distribution of podocyte proteins in 10-day-old 129 *Nphs2*$^{-/-}$ mice and age-matched controls. (a) Double immunolabeling and confocal microscopy on kidneys from *Nphs2*$^{+/+}$ and *Nphs2*$^{-/-}$ mice, with anti-nephrin (in green) and anti-nidogen (in red) antibodies. The anti-nidogen antibody gives a strong linear labeling of the GBM in wild-type and knockout mice. In the wild-type mice, nephrin is regularly distributed along the GBM, and there is a nearly complete superposition of the green linear labeling with anti-nephrin antibodies and the red linear labeling of the GBM. Nephrin labeling in knockout mice is granular and irregularly scattered at distance of the red GBM labeling. (b) Immunofluorescence analysis of ZO1, CD2AP, synaptopodin and α3-integrin. The expression of ZO1 and CD2AP is higher in *Nphs2*$^{-/-}$ mice than in controls, whereas the expression of synaptopodin and α3-integrin is unchanged.

cannot rule out the possibility that different genes (at least one in C57BL/6 and one in 129/Sv) act in a recessive way and modify (slow down) the progression of the disease in either pure of these genetic backgrounds. To test this hypothesis, we are currently backcrossing B6/129 mice on the C57BL/6 background. The localization and the characterization of these modifying loci will provide additional insights into the pathogenesis of glomerular diseases caused by podocyte injuries and may lead to the development of novel prophylactic or therapeutic approaches.

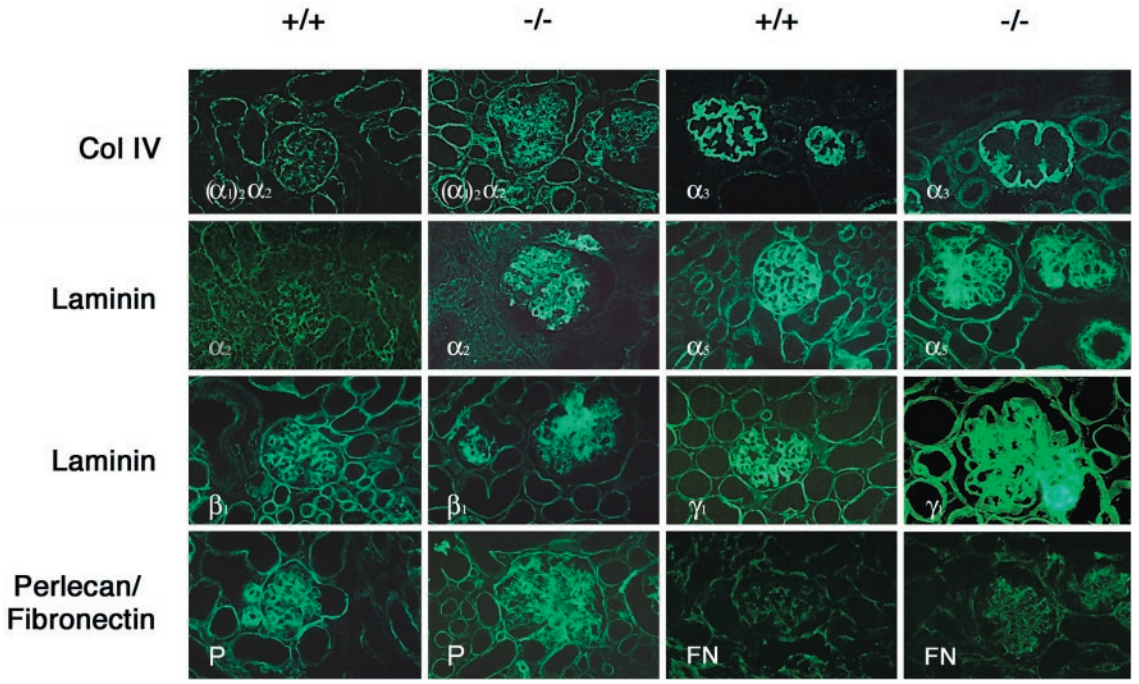

FIG. 6. Immunohistochemical analysis of the distribution of extracellular matrix proteins in 6-day-old *Nphs2*$^{-/-}$ B6/129 mice and age-matched controls. Increased mesangial expression of type IV collagen [α1(IV)2 α2(IV)], laminin α2, β1, and γ1 chains, perlecan, and fibronectin can be observed in *Nphs2*$^{-/-}$ mice associated with abnormal mesangial expression of the laminin α5 chain. The collagen α3(IV) chain remains restricted to the GBM, which appears to be pushed away by the mesangial expansion.

ACKNOWLEDGMENTS

We thank Marco Giovannini for providing the targeting vector and Karl Tryggvason, Richard Hynes, Peter Yurchenco, and Jeffrey Miner for the gifts of nephrin, α3-integrin, laminin α2, and laminin α5 antibodies, respectively. We are grateful to Joanna Lipecka, Brahim Delamain, and Yves Deris for assistance with confocal microscopy and photography. We thank Rosa Vargas for thoughtful help with statistical analysis and are grateful to Sandra Irrgang and Clemens Cohen for excellent assistance with the real-time PCR analysis.

This study was supported by the Association Claude Bernard; the Association pour l'Utilisation du Rein Artificiel; the Ministère de l'Education Nationale, de la Recherche, et de la Technologie; and the Fondation pour la Recherche Médicale (Ph.D. grants to S.R.). Funding to M.K. was provided by DFG Kr1492/6-3 and DHGP 01KW9922/2.

REFERENCES

1. **Andrews, K. L., J. L. Mudd, C. Li, and J. H. Miner.** 2002. Quantitative trait loci influence renal disease progression in a mouse model of Alport syndrome. Am. J. Pathol. **160:**721–730.
2. **Bidani, A. K., K. A. Griffin, W. Plott, and M. M. Schwartz.** 1993. Genetic predisposition to hypertension and microvascular injury in the remnant kidney model. J. Lab. Clin. Med. **122:**284–291.
3. **Boute, N., O. Gribouval, S. Roselli, F. Benessy, H. Lee, A. Fuchshuber, K. Dahan, M. C. Gubler, P. Niaudet, and C. Antignac.** 2000. NPHS2, encoding the glomerular protein podocin, is mutated in autosomal recessive steroid-resistant nephrotic syndrome. Nat. Genet. **24:**349–354.
4. **Cai, Y., A. Beziau, M. Sich, M. M. Kleppel, and M. C. Gubler.** 1996. Collagen distribution in human membranous glomerulonephritis. Pediatr. Nephrol. **10:**14–21.
5. **Caridi, G., R. Bertelli, A. Carrea, M. Di Duca, P. Catarsi, M. Artero, M. Carraro, C. Zennaro, G. Candiano, L. Musante, M. Seri, F. Ginevri, F. Perfumo, and G. M. Ghiggeri.** 2001. Prevalence, genetics, and clinical features of patients carrying podocin mutations in steroid-resistant nonfamilial focal segmental glomerulosclerosis. J. Am. Soc. Nephrol. **12:**2742–2746.
6. **Caridi, G., R. Bertelli, M. Di Duca, M. Dagnino, F. Emma, A. Onetti Muda, F. Scolari, N. Miglietti, G. Mazzucco, L. Murer, A. Carrea, L. Massella, G. Rizzoni, F. Perfumo, and G. M. Ghiggeri.** 2003. Broadening the spectrum of diseases related to podocin mutations. J. Am. Soc. Nephrol. **14:**1278–1286.
7. **Cherqui, S., C. Sevin, G. Hamard, V. Kalatzis, M. Sich, M. O. Pequignot, K. Gogat, M. Abitbol, M. Broyer, M. C. Gubler, and C. Antignac.** 2002. Intralysosomal cystine accumulation in mice lacking cystinosin, the protein defective in cystinosis. Mol. Cell. Biol. **22:**7622–7632.
8. **Ciani, L., A. Patel, N. D. Allen, and C. ffrench-Constant.** 2003. Mice lacking the giant protocadherin mFAT1 exhibit renal slit junction abnormalities and a partially penetrant cyclopia and anophthalmia phenotype. Mol. Cell. Biol. **23**:3575–3582.
9. **Cohen, C. D., K. Frach, D. Schlondorff, and M. Kretzler.** 2002. Quantitative gene expression analysis in renal biopsies: a novel protocol for a high-throughput multicenter application. Kidney Int. **61:**133–140.
10. **D'Agati, V.** 1994. The many masks of focal segmental glomerulosclerosis. Kidney Int. **46:**1223–1241.
11. **Donoviel, D. B., D. D. Freed, H. Vogel, D. G. Potter, E. Hawkins, J. P. Barrish, B. N. Mathur, C. A. Turner, R. Geske, C. A. Montgomery, M. Starbuck, M. Brandt, A. Gupta, R. Ramirez-Solis, B. P. Zambrowicz, and D. R. Powell.** 2001. Proteinuria and perinatal lethality in mice lacking NEPH1, a novel protein with homology to NEPHRIN. Mol. Cell. Biol. **21:**4829–4836.
12. **Doublier, S., V. Ruotsalainen, G. Salvidio, E. Lupia, L. Biancone, P. G. Conaldi, P. Reponen, K. Tryggvason, and G. Camussi.** 2001. Nephrin redistribution on podocytes is a potential mechanism for proteinuria in patients with primary acquired nephrotic syndrome. Am. J. Pathol. **158:**1723–1731.
13. **Esposito, C., C. J. He, G. E. Striker, R. K. Zalups, and L. J. Striker.** 1999. Nature and severity of the glomerular response to nephron reduction is strain-dependent in mice. Am. J. Pathol. **154:**891–897.
14. **Frishberg, Y., C. Rinat, O. Megged, E. Shapira, S. Feinstein, and A. Raas-Rothschild.** 2002. Mutations in NPHS2 encoding podocin are a prevalent cause of steroid-resistant nephrotic syndrome among Israeli-Arab children. J. Am. Soc. Nephrol. **13:**400–405.
15. **Furness, P. N., L. L. Hall, J. A. Shaw, and J. H. Pringle.** 1999. Glomerular expression of nephrin is decreased in acquired human nephrotic syndrome. Nephrol. Dial. Transplant. **14:**1234–1237.
16. **Grond, J., J. Y. Beukers, M. S. Schilthuis, J. J. Weening, and J. D. Elema.** 1986. Analysis of renal structural and functional features in two rat strains with a different susceptibility to glomerular sclerosis. Lab. Investig. **54:**77–83.
17. **Guo, J. K., A. L. Menke, M. C. Gubler, A. R. Clarke, D. Harrison, A. Hammes, N. D. Hastie, and A. Schedl.** 2002. WT1 is a key regulator of podocyte function: reduced expression levels cause crescentic glomerulonephritis and mesangial sclerosis. Hum. Mol. Genet. **11:**651–659.
18. **Hall, B. V.** 1955. Further studies of the normal structure of the renal glomerulus, p. 1–39. *In* Proceedings of the Sixth Annual Conference on Nephrotic Syndrome. National Kidney Foundation, New York, N.Y.

19. **Hammes, A., J. K. Guo, G. Lutsch, J. R. Leheste, D. Landrock, U. Ziegler, M. C. Gubler, and A. Schedl.** 2001. Two splice variants of the Wilms' tumor 1 gene have distinct functions during sex determination and nephron formation. Cell **106:**319–329.
20. **He, C., C. Esposito, C. Phillips, R. K. Zalups, D. A. Henderson, G. E. Striker, and L. J. Striker.** 1996. Dissociation of glomerular hypertrophy, cell proliferation, and glomerulosclerosis in mouse strains heterozygous for a mutation (Os) which induces a 50% reduction in nephron number. J. Clin. Investig. **97:**1242–1249.
21. **Holzman, L. B., P. L. St. John, I. A. Kovari, R. Verma, H. Holthofer, and D. R. Abrahamson.** 1999. Nephrin localizes to the slit pore of the glomerular epithelial cell. Kidney Int. **56:**1481–1491.
22. **Huber, T. B., B. Hartleben, J. Kim, M. Schmidts, B. Schermer, A. Keil, L. Egger, R. L. Lecha, C. Borner, H. Pavenstadt, A. S. Shaw, G. Walz, and T. Benzing.** 2003. Nephrin and CD2AP associate with phosphoinositide 3-OH kinase and stimulate AKT-dependent signaling. Mol. Cell. Biol. **23:**4917–4928.
23. **Huber, T. B., M. Kottgen, B. Schilling, G. Walz, and T. Benzing.** 2001. Interaction with podocin facilitates nephrin signaling. J. Biol. Chem. **276:**41543–41546.
24. **Huber, T. B., M. Schmidts, P. Gerke, B. Schermer, A. Zahn, B. Hartleben, L. Sellin, G. Walz, and T. Benzing.** 2003. The carboxyl terminus of neph family members binds to the PDZ domain protein zonula occludens-1. J. Biol. Chem. **278:**13417–13421.
25. **Ichikawa, I., and A. Fogo.** 1996. Focal segmental glomerulosclerosis. Pediatr. Nephrol. **10:**374–391.
26. **Inoue, T., E. Yaoita, H. Kurihara, F. Shimizu, T. Sakai, T. Kobayashi, K. Ohshiro, H. Kawachi, H. Okada, H. Suzuki, I. Kihara, and T. Yamamoto.** 2001. FAT is a component of glomerular slit diaphragms. Kidney Int. **59:**1003–1012.
27. **Jeanpierre, C., E. Denamur, I. Henry, M. O. Cabanis, S. Luce, A. Cecille, J. Elion, M. Peuchmaur, C. Loirat, P. Niaudet, M. C. Gubler, and C. Junien.** 1998. Identification of constitutional WT1 mutations, in patients with isolated diffuse mesangial sclerosis, and analysis of genotype/phenotype correlations by use of a computerized mutation database. Am. J. Hum. Genet. **62:**824–833.
28. **Kanwar, Y. S., Z. Z. Liu, N. Kashihara, and E. I. Wallner.** 1991. Current status of the structural and functional basis of glomerular filtration and proteinuria. Semin. Nephrol. **11:**390–413.
29. **Karle, S. M., B. Uetz, V. Ronner, L. Glaeser, F. Hildebrandt, and A. Fuchshuber.** 2002. Novel mutations in NPHS2 detected in both familial and sporadic steroid-resistant nephrotic syndrome. J. Am. Soc. Nephrol. **13:**388–393.
30. **Kawachi, H., H. Koike, H. Kurihara, E. Yaoita, M. Orikasa, M. A. Shia, T. Sakai, T. Yamamoto, D. J. Salant, and F. Shimizu.** 2000. Cloning of rat nephrin: expression in developing glomeruli and in proteinuric states. Kidney Int. **57:**1949–1961.
31. **Kerjaschki, D.** 2001. Caught flat-footed: podocyte damage and the molecular bases of focal glomerulosclerosis. J. Clin. Investig. **108:**1583–1587.
32. **Kestila, M., U. Lenkkeri, M. Mannikko, J. Lamerdin, P. McCready, H. Putaala, V. Ruotsalainen, T. Morita, M. Nissinen, R. Herva, C. E. Kashtan, L. Peltonen, C. Holmberg, A. Olsen, and K. Tryggvason.** 1998. Positionally cloned gene for a novel glomerular protein—nephrin—is mutated in congenital nephrotic syndrome. Mol. Cell **1:**575–582.
33. **Kim, J. M., H. Wu, G. Green, C. A. Winkler, J. B. Kopp, J. H. Miner, E. R. Unanue, and A. S. Shaw.** 2003. CD2-associated protein haploinsufficiency is linked to glomerular disease susceptibility. Science **300:**1298–1300**.**
34. **Kos, C., T. Le, S. Sinha, J. Henderson, S. Kim, H. Sugimoto, R. Kalluri, R. Gerszten, and M. Pollak.** 2003. Mice deficient in alpha-actinin-4 have severe glomerular disease. J. Clin. Investig. **111:**1683–1690.
35. **Koziell, A., V. Grech, S. Hussain, G. Lee, U. Lenkkeri, K. Tryggvason, and P. Scambler.** 2002. Genotype/phenotype correlations of NPHS1 and NPHS2 mutations in nephrotic syndrome advocate a functional inter-relationship in glomerular filtration. Hum. Mol. Genet. **11:**379–388.
36. **Lahdenpera, J., P. Kilpelainen, X. L. Liu, T. Pikkarainen, P. Reponen, V. Ruotsalainen, and K. Tryggvason.** 2003. Clustering-induced tyrosine phosphorylation of nephrin by Src family kinases. Kidney Int. **64:**404–413.
37. **Lehtonen, S., F. Zhao, and E. Lehtonen.** 2002. CD2-associated protein directly interacts with the actin cytoskeleton. Am. J. Physiol. Renal Physiol. **283:**F734–F743.
38. **Li, C., V. Ruotsalainen, K. Tryggvason, A. S. Shaw, and J. H. Miner.** 2000. CD2AP is expressed with nephrin in developing podocytes and is found widely in mature kidney and elsewhere. Am. J. Physiol. Renal Physiol. **279:**F785–F792.
39. **Michaud, J. L., L. I. Lemieux, M. Dube, B. C. Vanderhyden, S. J. Robertson, and C. R. Kennedy.** 2003. Focal and segmental glomerulosclerosis in mice with podocyte-specific expression of mutant alpha-actinin 4. J. Am. Soc. Nephrol. **14:**1200–1211.
40. **Miner, J. H., R. Morello, K. L. Andrews, C. Li, C. Antignac, A. S. Shaw, and B. Lee.** 2002. Transcriptional induction of slit diaphragm genes by Lmx1b is required in podocyte differentiation. J. Clin. Investig. **109:**1065–1072.
41. **Mundel, P., and S. J. Shankland.** 2002. Podocyte biology and response to injury. J. Am. Soc. Nephrol. **13:**3005–3015.
42. **Ohashi, T., K. Uchida, S. Uchida, S. Sasaki, and H. Nihei.** 2003. Intracellular mislocalization of mutant podocin and correction by chemical chaperones. Histochem. Cell Biol. **119:**257–264.
43. **Ohishi, A., H. Suzuki, H. Nakamoto, H. Katsumata, K. Hayashi, M. Ryuzaki, K. Kumagai, T. Furukawa, A. Ichihara, T. Saruta, et al.** 1995. Status of patients who underwent uninephrectomy in adulthood more than 20 years ago. Am. J. Kidney Dis. **26**:889–897.
44. **Pelletier, J., W. Bruening, F. P. Li, D. A. Haber, T. Glaser, and D. E. Housman.** 1991. WT1 mutations contribute to abnormal genital system development and hereditary Wilms' tumour. Nature **353:**431–434.
45. **Rantanen, M., T. Palmen, A. Patari, H. Ahola, S. Lehtonen, E. Astrom, T. Floss, F. Vauti, W. Wurst, P. Ruiz, D. Kerjaschki, and H. Holthofer.** 2002. Nephrin TRAP mice lack slit diaphragms and show fibrotic glomeruli and cystic tubular lesions. J. Am. Soc. Nephrol. **13:**1586–1594.
46. **Reiser, J., W. Kriz, M. Kretzler, and P. Mundel.** 2000. The glomerular slit diaphragm is a modified adherens junction. J. Am. Soc. Nephrol. **11:**1–8.
47. **Rohr, C., J. Prestel, L. Heidet, H. Hosser, W. Kriz, R. L. Johnson, C. Antignac, and R. Witzgall.** 2002. The LIM-homeodomain transcription factor Lmx1b plays a crucial role in podocytes. J. Clin. Investig. **109:**1073–1082.
48. **Roselli, S., O. Gribouval, N. Boute, M. Sich, F. Benessy, T. Attie, M. C. Gubler, and C. Antignac.** 2002. Podocin localizes in the kidney to the slit diaphragm area. Am. J. Pathol. **160:**131–139.

48a. **Roselli, S., I. Nautkine, O. Gribouval, A. Benmerah, and C. Antignac.** Plasma membrane targeting of podocin through the classical exocytic pathway: effect of NPHS2 mutations. Traffic, in press.

49. **Ruotsalainen, V., P. Ljungberg, J. Wartiovaara, U. Lenkkeri, M. Kestila, H. Jalanko, C. Holmberg, and K. Tryggvason.** 1999. Nephrin is specifically located at the slit diaphragm of glomerular podocytes. Proc. Natl. Acad. Sci. USA **96:**7962–7967.
50. **Schnabel, E., J. M. Anderson, and M. G. Farquhar.** 1990. The tight junction protein ZO-1 is concentrated along slit diaphragms of the glomerular epithelium. J. Cell Biol. **111:**1255–1263.
51. **Schwarz, K., M. Simons, J. Reiser, M. A. Saleem, C. Faul, W. Kriz, A. S. Shaw, L. B. Holzman, and P. Mundel.** 2001. Podocin, a raft-associated component of the glomerular slit diaphragm, interacts with CD2AP and nephrin. J. Clin. Investig. **108:**1621–1629.
52. **Sellin, L., T. B. Huber, P. Gerke, I. Quack, H. Pavenstadt, and G. Walz.** 2003. NEPH1 defines a novel family of podocin interacting proteins. FASEB J. **17:**115–117.
53. **Shih, N. Y., J. Li, R. Cotran, P. Mundel, J. H. Miner, and A. S. Shaw.** 2001. CD2AP localizes to the slit diaphragm and binds to nephrin via a novel C-terminal domain. Am. J. Pathol. **159:**2303–2308.
54. **Shih, N. Y., J. Li, V. Karpitskii, A. Nguyen, M. L. Dustin, O. Kanagawa, J. H. Miner, and A. S. Shaw.** 1999. Congenital nephrotic syndrome in mice lacking CD2-associated protein. Science **286:**312–315.
55. **Simons, M., K. Schwarz, W. Kriz, A. Miettinen, J. Reiser, P. Mundel, and H. Holthofer.** 2001. Involvement of lipid rafts in nephrin phosphorylation and organization of the glomerular slit diaphragm. Am. J. Pathol. **159:**1069–1077.
56. **te Riele, H., E. Maandag, A. Clarke, M. Hooper, and A. Berns.** 1990. Consecutive inactivation of both alleles of the pim-1 proto-oncogene by homologous recombination in embryonic stem cells. Nature **13:**649–651.
57. **Tsukaguchi, H., A. Sudhakar, T. C. Le, T. Nguyen, J. Yao, J. A. Schwimmer, A. D. Schachter, E. Poch, P. F. Abreu, G. B. Appel, A. B. Pereira, R. Kalluri, and M. R. Pollak.** 2002. NPHS2 mutations in late-onset focal segmental glomerulosclerosis: R229Q is a common disease-associated allele. J. Clin. Investig. **110:**1659–1666.
58. **Verma, R., B. Wharram, I. Kovari, R. Kunkel, D. Nihalani, K. K. Wary, R. C. Wiggins, P. Killen, and L. B. Holzman.** 2003. Fyn binds to and phosphorylates the kidney slit diaphragm component nephrin. J. Biol. Chem. **278:**20716–20723.
59. **Yuan, H., E. Takeuchi, and D. J. Salant.** 2002. Podocyte slit-diaphragm protein nephrin is linked to the actin cytoskeleton. Am. J. Physiol. Renal Physiol. **282:**F585–F591.
60. **Yuan, H., E. Takeuchi, G. A. Taylor, M. McLaughlin, D. Brown, and D. J. Salant.** 2002. Nephrin dissociates from actin, and its expression is reduced in early experimental membranous nephropathy. J. Am. Soc. Nephrol. **13:**946–956.
61. **Zheng, F., G. E. Striker, C. Esposito, E. Lupia, and L. J. Striker.** 1998. Strain differences rather than hyperglycemia determine the severity of glomerulosclerosis in mice. Kidney Int. **54:**1999–2007.